

Density of states and dynamic scaling on the Vicsek snowflake fractal

This article has been downloaded from IOPscience. Please scroll down to see the full text article.

1988 J. Phys. A: Math. Gen. 21 2431

(<http://iopscience.iop.org/0305-4470/21/10/020>)

View [the table of contents for this issue](#), or go to the [journal homepage](#) for more

Download details:

IP Address: 129.252.86.83

The article was downloaded on 01/06/2010 at 05:36

Please note that [terms and conditions apply](#).

Density of states and dynamic scaling on the Vicsek snowflake fractal

J A Ashraff† and B W Southern

Department of Physics, University of Manitoba, Winnipeg, Manitoba, Canada R3T 2N2

Received 10 August 1987, in final form 9 February 1988

Abstract. Real-space rescaling techniques have been employed to obtain recursion relations for the parameters characterising the dynamics of both the Heisenberg ferromagnet and antiferromagnet on the infinite Vicsek snowflake fractal. We have calculated the associated dynamic exponents z_F and z_A by linearising about the respective fixed points of the ferromagnetic/antiferromagnetic recursion relations and find them to satisfy the relation $z_A = z_F/2$. In addition, using a functional integral method both the ferromagnetic and antiferromagnetic density of states $\rho_F(\omega)$ and $\rho_A(\omega)$ have been calculated exactly and the resulting spectra were found to satisfy the scaling equation $\rho_\alpha(\omega) \sim b^{z_\alpha - d_f} \rho(\lambda_\alpha \omega)$ near their respective fixed points ($\alpha = A, F$), d_f denoting the fractal dimension. Finally, the amplitudes $g_\alpha(\omega)$ appearing in the solution to the scaling equation $\rho_\alpha(\omega) \sim g_\alpha(\omega) \omega^{d_f/z_\alpha - 1}$, for the density of states $\rho_\alpha(\omega)$, were found to be periodic functions of $\ln(\omega)$ with period $\ln(\lambda_\alpha)$ where λ_α is the eigenvalue associated with ferromagnetic ($\alpha = F$) or antiferromagnetic ($\alpha = A$) fixed point.

1. Introduction

During the past several years much work has been done on modelling disordered systems using geometric shapes of fractal dimension called fractals (Mandelbrot 1982). Fractals were introduced within the context of percolation by Stanley (1977) and have subsequently served as models for the geometry of such inhomogeneous systems as metal-insulator thin films, gels and dilute spin systems. As models of disorder, fractals have several favourable attributes, most notably their non-uniformity and self-similarity, a direct result of the way in which they are constructed. Indeed, it is this same intrinsic self-similarity that makes fractals ideally suited to be treated using length scaling techniques (Stinchcombe 1985).

The dynamics of spin systems on fractals involves at least three different dimensions for its description: the Euclidean dimension d , the fractal dimension d_f (Mandelbrot 1982) and the spectral dimension d_s (Alexander and Orbach 1982). The latter two dimensions characterise how the mass (or number of spins) of the system scales with size and how the spectral properties of a given Hamiltonian on this fractal geometry scale with frequency or energy. Previous work on exact fractals has focused mainly on the Sierpinski gasket and has included studies of the electronic (Tremblay and Southern 1983), dynamical (Rammal 1984, Maggs and Stinchcombe 1986, Friedberg and Martin 1986) and static (Gefen *et al* 1981) properties. In this paper we study the dynamics of both the Heisenberg ferromagnet and antiferromagnet on the Vicsek

† Present address: Department of Theoretical Physics, University of Oxford, 1 Keble Road, Oxford OX1 3NP, UK.

snowflake fractal. This fractal was first introduced by Vicsek (1983) as a model for aggregation phenomena, but we shall use it to describe the positions of spins in space. The Vicsek snowflake is constructed by taking a square of side a and dividing it into nine smaller squares of side $a/3$, four of which are then discarded, the process then being repeated in each of the remaining squares ad infinitum. Figure 1 illustrates the situation after two levels of decoration.

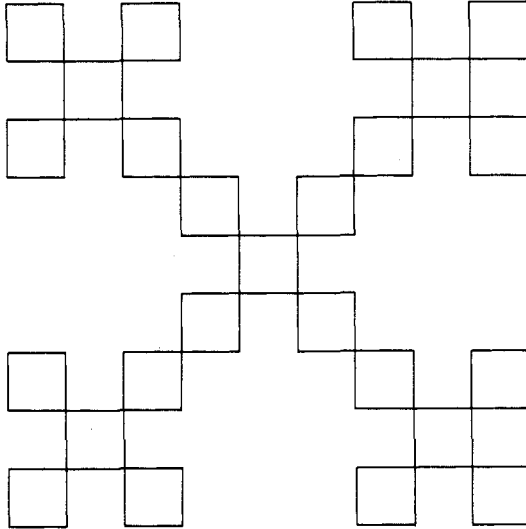


Figure 1. The Vicsek snowflake fractal decorated to two levels.

The motivation for the present work was to investigate whether the relationship $z_A = z_F/2$, between the dynamic exponents z_F and z_A for the Heisenberg ferromagnet and antiferromagnet, which holds for regular Euclidean lattices, also holds for bond diluted, non-uniform lattices. To model the bond dilution we have used the (non-uniform) Vicsek fractal which not only allows for both ferromagnetic and antiferromagnetic orderings of the spins but also does not suffer from the frustration effects inherent in the triangular-shaped Sierpinski gasket fractal. In this paper we present the results of a calculation of the critical exponents z_F and z_A associated with (Heisenberg) ferromagnetic and antiferromagnetic spin-wave dynamics on the same fractal lattice. From a fixed-point analysis of the recursion relations generated by decimating the spin-wave equations of motion we have found these exponents to satisfy the relation $z_A = z_F/2$ (Stinchcombe and Maggs 1986) as is found for ordinary Euclidean lattices. In addition, using length-scaling techniques combined within a generating function formalism we have performed an exact calculation of the density of both ferromagnetic and antiferromagnetic spin-wave states $\rho_F(\omega)$ and $\rho_A(\omega)$ respectively and have found the resulting spectra to obey the following basic scaling form:

$$\rho_\alpha(\omega) \sim b^{z_\alpha - d_s} \rho_\alpha(\lambda_\alpha \omega) \quad (1.1)$$

where $\lambda_\alpha = b^{z_\alpha}$ is the largest eigenvalue associated with the fixed point of the appropriate rescaling transformation, b is the rescaling factor ($b=3$) and z_α is the dynamic exponent. The spectral dimension d_s is then obtained from $d_s = 2d_f/z_\alpha$. It must be emphasised that the spectral dimension d_s is the relevant exponent describing the

behaviour of the low-frequency density of states, the fractal dimension d_f alone being insufficient.

2. Ferromagnetic spin waves on the Vicsek snowflake

Consider a system of Heisenberg spins occupying the sites of the Vicsek snowflake geometry, each coupled to its nearest and next-nearest neighbours through ferromagnetic exchange interactions J_1 and J_2 respectively. The dynamics of the i th transverse spin component S_i^+ is determined by Heisenberg's equation of motion leading to

$$\left(\sum_j J_{ij} - \omega\right)S_i^+ = \sum_j J_{ij}S_j^+ \tag{2.1}$$

where the sums are taken over both nearest and next-nearest neighbours of i and $J_{ij} = J_1(J_2)$ if j is a nearest (next-nearest) neighbour of i . Although we have focused only on spin-wave dynamics, the equation of motion (2.1) is formally identical to that which one would obtain if discussing harmonic excitations (phonons), tight-binding electrons, random walks and diffusion, and so the results presented here clearly apply to a wide range of phenomena.

In order to maintain the form (2.1) it is necessary to scale the quantity $z_1J_1 + z_2J_2$ independently of J_1 and J_2 (z_1 and z_2 denote the number of nearest and next-nearest neighbours respectively) and it is thus convenient to define

$$K_2 = 2J_1 + J_2 \qquad K_4 = 4J_1 + 2J_2. \tag{2.2}$$

The decimation procedure involves the elimination of the interior twelve sites leading to equations for the remaining four sites which are again of the form (2.1) but with renormalised parameters J'_1, J'_2, K'_2 , and K'_4 . It should be pointed out that to obtain a truly general set of recursion relations it is necessary to include next-nearest neighbour interactions from the very outset since the elimination process generates them (Niemeijer and van Leeuwen 1976). Such a proliferation of interactions is, however, only restricted to second neighbours and does not increase beyond this in contrast to the situation that arises when decimation is applied to regular Euclidean lattices in two and three dimensions (Southern and Loly 1985).

Introducing the dimensionless variables X, Y , and Z defined by

$$X = (K_2 - \omega)/J_1 \qquad Y = (K_4 - \omega)/J_1 \qquad Z = J_2/J_1 \tag{2.3}$$

leads to the form of the recursion relations given in appendix 1. This three-parameter map possesses six fixed points; however, since we are primarily interested in low-frequency excitations only the fixed point $(X^*, Y^*, Z^*) = (3, 6, 1)$, corresponding to $\omega = 0$, is of relevance. Linearising about this fixed point leads to a largest eigenvalue λ_F of 15 and hence a dynamic exponent $z_F = \ln 15/\ln 3$ and a spectral dimension $d_s = 2 \ln 5/\ln 15$. Guyer (1984) has studied the random walk problem on this same fractal and obtained the same result for the spectral dimension, as is to be expected, due to the mathematical equivalence between the equations describing ferromagnetic spin waves and random walks. Note also that the exponent z_F can also be obtained from scaling a static quantity such as the conductivity and employing the relation $z_F = d_f + \hat{t}$ (Given and Mandelbrot 1983, Christou and Stinchcombe 1985) where d_f is the fractal dimension and \hat{t} the conductivity exponent ($d_f = \ln 5/\ln 3, \hat{t} = 1$).

The density of states $\rho(\omega)$ has been calculated using the following (complex) generating function $\mathcal{F}(\omega)$ (Tremblay and Southern 1983, Lavis *et al* 1985, Southern and Douchant 1985, Ashraff 1986, Maggs and Stinchcombe 1986):

$$\mathcal{F}(\omega) = \ln \left(\int \mathcal{D}S \exp\left(\frac{1}{2}i\mathcal{A}(\omega)\right) \right) \quad (2.4)$$

where

$$\mathcal{A}(\omega) = \sum_i (\omega + i\eta - K_i) S_i^2 - \sum_{ij} J_{ij} S_i S_j \quad (2.5)$$

and

$$\int \mathcal{D}S = \prod_i \int_{-\infty}^{+\infty} dS_i \quad (2.6)$$

with $K_i = \sum_j J_{ij}$ and the small imaginary part η ensures convergence of the integrals. One then obtains $\rho(\omega)$ using

$$\rho(\omega) = \frac{2}{\pi} \Im \left(\frac{\partial \mathcal{F}(\omega)}{\partial \omega} \right) \quad (2.7)$$

where \Im denotes the imaginary part. Our calculation of $\rho(\omega)$ based on (2.7) involves the recursive evaluation of the generating function $\mathcal{F}(\omega)$ using the technique of the real-space renormalisation group (RSRG). The idea behind such an RSRG calculation involves successively performing the Gaussian integrals appearing in (2.4), corresponding to the elimination of sites. To facilitate this process it is convenient to partition the lattice of sites into two sublattices \mathcal{L}_1 and \mathcal{L}_2 corresponding to those sites which are to remain and to be eliminated respectively at stage n of the elimination process. Then performing the Gaussian integrals over \mathcal{L}_2 leads to a constant term and a generating function \mathcal{F} describing a system with a fraction of the original degrees of freedom, involving an action of the same form as (2.5) but with new parameters K'_i and J'_{ij} which, when written in the dimensionless form (2.3), take the form given in appendix 1. Continuing on in this fashion and accumulating the constant terms numerically, arising from the Gaussian integration, at each stage, we are led to $\mathcal{F}(\omega)$ and hence $\rho_F(\omega)$ via (2.7). We refer the reader to the papers of Tremblay and Southern (1983) and Lavis *et al* (1985) for details. Figure 2 shows the ferromagnetic density of states $\rho_F(\omega)$ obtained using the initial conditions $J_1 = 1$, $J_2 = 0$, $K_2 = 2$, and $K_4 = 4$. The spectrum $\rho_F(\omega)$ is obviously highly singular and consists of a series of peaks and gaps, whose width is due to the finite imaginary part in the frequency, and which give rise to the devil's staircase form for the integrated density of states $N_F(\omega)$ (Rammal 1984). Near the fixed point at $\omega = 0$ it can be shown from (2.4) that the density of states has the scaling form (Niemeijer and van Leeuwen 1976)

$$\rho_F(\omega) \sim b^{z_F - d_t} \rho_F(\lambda_F \omega) \quad (2.8)$$

which we have verified numerically, using the eigenvalue λ_F and dynamic exponent z_F obtained from the fixed-point analysis. The most general solution to (2.8) takes the form

$$\rho_F(\omega) \sim \omega^{(d_t - z_F)/z_F} g_F(\omega) \quad (2.9)$$

where the amplitude $g_F(\omega)$ satisfies

$$g_F(\omega) = g_F(\lambda_F \omega). \quad (2.10)$$

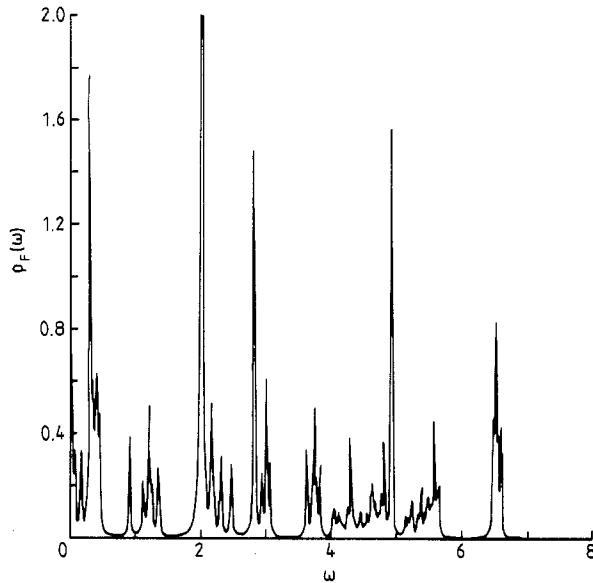


Figure 2. The ferromagnetic spin-wave density of states with $J_1 = 1$ and $J_2 = 0$.

Equation (2.10) predicts that a plot of $\ln \rho\omega$ against $\ln \omega$ should yield a straight line upon which is superimposed a periodic amplitude of period $\ln \lambda_F$, and referring to figure 3 we see that this is indeed the case. This plot was obtained using a uniform density of $\ln \omega$ points leading to a non-uniform density of ω points and hence resulting in the resolution being non-uniform. Such periodicities do not occur when the lattice is translationally invariant because an arbitrary scaling factor b can be used. However,

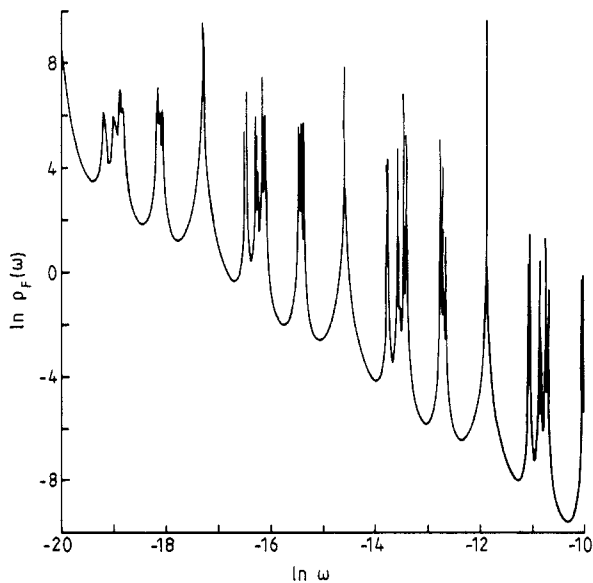


Figure 3. A \ln - \ln plot of the ferromagnetic spin-wave density of states against frequency near $\omega = 0$ with $J_1 = 1$ and $J_2 = 0$.

for non-random fractals the choice of b is fixed and oscillatory amplitudes are expected in the spectral properties (Niemeijer and van Leeuwen 1976, Bessis *et al* 1983, Knezevic and Southern 1986, Maggs and Stinchcombe 1986, Southern and Knezevic 1987, Stinchcombe 1987).

3. Antiferromagnetic spin waves on the Vicsek snowflake

We now consider the situation where the sites of the Vicsek snowflake form two interpenetrating sublattices \mathcal{L}_A and \mathcal{L}_B , the spins alternating from up to down on adjacent sites. Whereas in § 2 it was only necessary to distinguish between two types of sites and two interactions it will be necessary in the case of the antiferromagnet to distinguish between four types of sites and three types of interactions.

The linearised Heisenberg equation of motion for the transverse component S_i^+ is now given by

$$\left(\omega + \sum_j (-1)^{\beta_j} J_{ij}\right) S_i^+ = (-1)^{\beta_i} \sum_j J_{ij} S_j^+ \quad (3.1)$$

where $\beta_r = 1$ if $r \in \mathcal{L}_A$ and $\beta_r = 2$ if $r \in \mathcal{L}_B$. We now define

$$K_{2A} = 2J_1 - J_{2A} \quad K_{2B} = 2J_1 - J_{2B} \quad (3.2a)$$

$$K_{4A} = 4J_1 - 2J_{2A} \quad K_{4B} = 4J_1 - 2J_{2B}. \quad (3.2b)$$

As in the ferromagnetic case the decimation procedure consists of eliminating the interior twelve sites leading to renormalised parameters $J'_1, J'_{2A}, J'_{2B}, K'_{2A}, K'_{2B}, K'_{4A}, K'_{4B}$. It is again convenient to define a set of dimensionless quantities which in the present case take the form

$$X_A = (\omega - K_{2A})/J_1 \quad X_B = (-\omega - K_{2B})/J_1 \quad (3.3a)$$

$$Y_A = (\omega - K_{4A})/J_1 \quad Y_B = (-\omega - K_{4B})/J_1 \quad (3.3b)$$

$$Z_A = J_{2A}/J_1 \quad Z_B = J_{2B}/J_1 \quad (3.3c)$$

(the recursion relations then take the form given in appendix 2 with the fixed point of interest now being $(X_A^*, \dots, Z_B^*) = (-3, -3, -6, -6, -1, -1)$. Although linearisation about this fixed point leads to an eigenvalue $\lambda_A = 15$, the scaling field is quadratic in ω to leading order (the linear terms cancelling) in contrast to the ferromagnetic case where to leading order the scaling field is linear in ω . The dynamic exponent z_A is thus given by $z_A = z_F/2 = \ln 15/\ln 9$ leading to a spectral dimension of $d_s = \ln 5/\ln 15$.

In figures 4 and 5 we show the antiferromagnetic spin wave DOS $\rho_A(\omega)$ and a ln-ln plot again displaying the periodicities predicted by (2.10). We have found that the spectra obey the same scaling equations (2.6) as the ferromagnetic spectra with z_F replaced by z_A .

4. Conclusions

In conclusion, we have presented an exact calculation of the dynamic exponents z_F and z_A associated with ferromagnetic and antiferromagnetic spin waves on the Vicsek

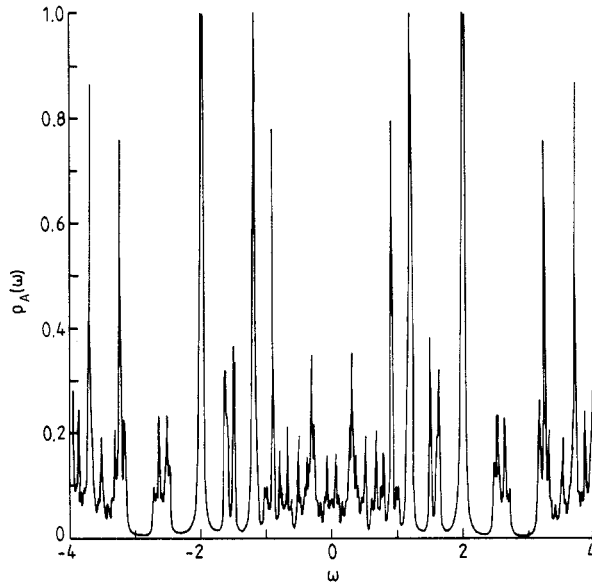


Figure 4. The antiferromagnetic spin-wave density of states with $J_{1A} = J_{1B} = 1$ and $J_{2A} = J_{2B} = 0$.

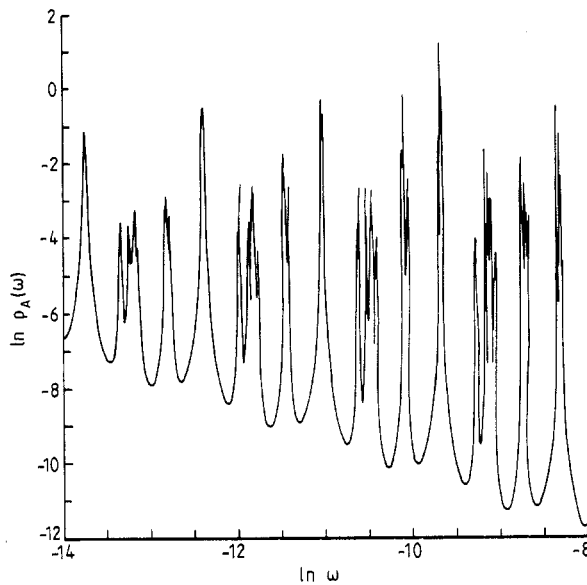


Figure 5. A \ln - \ln plot of the antiferromagnetic density of spin-wave states against frequency near $\omega = 0$ with $J_{1A} = J_{1B} = 1$ and $J_{2A} = J_{2B} = 0$.

snowflake fractal and have found them to satisfy the relation $z_A = z_F/2$, a result which may be valid only for fractals with well defined sublattices. In addition, the excitation spectra $\rho_\alpha(\omega)$ were calculated explicitly for both ferromagnetic and antiferromagnetic spin-wave excitations on the same fractal and found to have the basic form $\rho_\alpha(\omega) \sim g_\alpha(\omega)\omega^{(d/z_\alpha-1)}$ with $g_\alpha(\omega)$ periodic in $\ln \omega$ with period $\ln \lambda_\alpha$. It is worth commenting

that for a regular Euclidean object, any one of an infinite number of scale factors b may be used when performing a decimation and hence an equivalent number of corresponding eigenvalues λ_α are possible, indicating that (2.10) has only the solution $g_\alpha(\omega) = \text{constant}$. We would thus expect that a low-frequency plot of $\ln \rho(\omega)$ against $\ln \omega$ will yield a straight line of slope $1 - d/z_\alpha$ from which we may obtain the exponent z_α . This situation is quite different for an exact fractal such as the Sierpinski gasket or the Vicsek snowflake where there is a discrete (fixed) scale factor b . In this case the periodicities in the amplitude prevent one from obtaining z_α in the same way and so one is forced to employ a method based upon a fixed-point analysis as was described in this paper or alternatively a numerical scheme.

Acknowledgments

One of us (JAA) would like to thank Dr R B Stinchcombe for pointing out that the dynamic exponent z_F could be obtained by a simple static scaling of the conductance. This work was supported by the Natural Sciences and Engineering Research Council of Canada.

Appendix 1. Ferromagnetic recursion relations

The recursion relations for the parameters X , Y , and Z defined in § 2 are given by

$$X' = \frac{X}{\Phi R^2} - \frac{2}{(X-Z)\Phi R^2} - \frac{\Lambda}{\Phi} \quad (\text{A1.1})$$

$$Y' = \frac{Y}{\Phi R^2} - \frac{4}{(X-Z)\Phi R^2} - \frac{2\Lambda}{\Phi} \quad (\text{A1.2})$$

$$Z' = \Psi/\Phi \quad (\text{A1.3})$$

where

$$\Lambda = \frac{Q(Q-Z)-2}{(Q+Z)[(Q-Z)^2-4]} \quad (\text{A1.4})$$

$$\Phi = \frac{1}{(Q-Z)^2-4} \quad (\text{A1.5})$$

$$\Psi = \frac{2+Z(Q-Z)}{(Q+Z)[(Q-Z)^2-4]} \quad (\text{A1.6})$$

and

$$Q = Y - 2/(X - Z) \quad (\text{A1.7})$$

$$R = Z + 2/(X - Z). \quad (\text{A1.8})$$

Appendix 2. Antiferromagnetic recursion relations

The recursion relations for the parameters $X_A, X_B, Y_A, Y_B, Z_A,$ and Z_B are given by

$$X'_A = \frac{X_A}{\Phi R_A R_B} - \frac{2}{\Phi R_A R_B (X_B - Z_B)} - \frac{\Delta_A R_A}{\Phi R_B} \tag{A2.1}$$

$$X'_B = \frac{X_B}{\Phi R_A R_B} - \frac{2}{\Phi R_A R_B (X_A - Z_A)} - \frac{\Lambda_B R_B}{\Phi R_A} \tag{A2.2}$$

$$Y'_A = \frac{Y_A}{\Phi R_A R_B} - \frac{4}{\Phi R_A R_B (X_B - Z_B)} - \frac{2\Lambda_A R_A}{\Phi R_B} \tag{A2.3}$$

$$Y'_B = \frac{Y_B}{\Phi R_A R_B} - \frac{4}{\Phi R_A R_B (X_A - Z_A)} - \frac{2\Lambda_B R_B}{\Phi R_A} \tag{A2.4}$$

$$Z'_A = \frac{\Psi_A R_A}{\Phi R_B} \tag{A2.5}$$

$$Z'_B = \frac{\Psi_B R_B}{\Phi R_A} \tag{A2.6}$$

where

$$\Lambda_A = \frac{Q_A(Q_B - Z_B) - 2}{(Q_A + Z_A)[(Q_A - Z_A)(Q_B - Z_B) - 4]} \tag{A2.7}$$

$$\Lambda_B = \frac{Q_B(Q_A - Z_A) - 2}{(Q_B + Z_B)[(Q_A - Z_A)(Q_B - Z_B) - 4]} \tag{A2.8}$$

$$\Phi = \frac{1}{(Q_A - Z_A)(Q_B - Z_B) - 4} \tag{A2.9}$$

$$\Psi_A = \frac{2 + Z_A(Q_B - Z_B)}{(Q_A + Z_A)[(Q_A - Z_A)(Q_B - Z_B) - 4]} \tag{A2.10}$$

$$\Psi_B = \frac{2 + Z_B(Q_A - Z_A)}{(Q_B + Z_B)[(Q_A - Z_A)(Q_B - Z_B) - 4]} \tag{A2.11}$$

and

$$Q_A = Y_A - \frac{2}{X_B - Z_B} \quad Q_B = Y_B - \frac{2}{X_A - Z_A} \tag{A2.12}$$

$$R_A = Z_A + \frac{2}{X_B - Z_B} \quad R_B = Z_B + \frac{2}{X_A - Z_A} \tag{A2.13}$$

References

Alexander S and Orbach R 1982 *J. Physique Lett.* **43** L625
 Ashraff J A 1986 *MSc thesis* University of Manitoba
 Bessis D, Geronimo J S and Moussa P 1983 *J. Physique Lett.* **44** L977
 Christou A and Stinchcombe R B 1986 *J. Phys. A: Math. Gen.* **19** 2625

- Friedberg R and Martin O 1986 *J. Physique* **47** 1663
Gefen V, Mandelbrot B B and Aharony A 1980 *Phys. Rev. Lett.* **45** 855
Given J A and Mandelbrot B B 1983 *J. Phys. A: Math. Gen.* **16** L565
Guyer R A 1984 *Phys. Rev. A* **30** 1112
Knezevic M and Southern B W 1986 *Phys. Rev. B* **34** 4966
Lavis D A, Southern B W and Davison S G 1985 *J. Phys. C: Solid State Phys.* **18** 1387
Maggs A C and Stinchcombe R B 1986 *J. Phys. A: Math. Gen.* **19** 398
Mandelbrot B B 1982 *The Fractal Geometry of Nature* (San Francisco: Freeman)
Niemeijer T and van Leeuwen J M J 1976 *Phase Transitions and Critical Phenomena* vol 6, ed C Domb and M S Green (New York: Academic) p 425
Rammal R 1984 *J. Physique* **45** 191
Southern B W and Douchant A R 1985 *Phys. Rev. Lett.* **55** 966
Southern B W and Knezevic M 1987 *Phys. Rev. B* **35** 5036
Southern B W and Loly P D 1985 *J. Phys. A: Math. Gen.* **18** 525
Stanley H E 1977 *J. Phys. A: Math. Gen.* **10** L211
Stinchcombe R B 1985 *Scaling Phenomena in Disordered Systems* ed R Pynn and A Skjeltorp (New York: Plenum)
—— 1987 *J. Phys. A: Math. Gen.* **20** L251
Stinchcombe R B and Maggs A C 1986 *J. Phys. A: Math. Gen.* **19** 1949
Tremblay A M S and Southern B W 1983 *J. Physique Lett.* **44** L843
Vicsek T 1983 *J. Phys. A: Math. Gen.* **16** L647